Cell Death and Differentiation (2012) 19, 692–702

www.nature.com/cdd

# RP58/ZNF238 directly modulates proneurogenic gene levels and is required for neuronal differentiation and brain expansion

C Xiang[1], V Baubet[1], S Pal[1], L Holderbaum[1], V Tatard[1], P Jiang[1], RV Davuluri[1] and N Dahmane*[,1]

**Although neurogenic pathways have been described in the developing neocortex, less is known about mechanisms ensuring correct neuronal differentiation thus also preventing tumor growth. We have shown that *RP58* (aka *zfp238* or *znf238*) is highly expressed in differentiating neurons, that its expression is lost or diminished in brain tumors, and that its reintroduction blocks their proliferation. Mice with loss of *RP58* die at birth with neocortical defects. Using a novel conditional *RP58* allele here we show that its CNS-specific loss yields a novel postnatal phenotype: microencephaly, agenesis of the corpus callosum and cerebellar hypoplasia that resembles the chr1qter deletion microcephaly syndrome in human. *RP58* mutant brains maintain precursor pools but have reduced neuronal and increased glial differentiation. Well-timed downregulation of *pax6*, *ngn2* and *neuroD1* depends on RP58 mediated transcriptional repression, *ngn2* and *neuroD1* being direct targets. Thus, RP58 may act to favor neuronal differentiation and brain growth by coherently repressing multiple proneurogenic genes in a timely manner.**
*Cell Death and Differentiation* (2012) **19,** 692–702; doi:10.1038/cdd.2011.144; published online 18 November 2011

The cerebral cortex undergoes rapid expansion during embryogenesis, when neuronal layers are formed. Two main types of precursors exist in the developing neocortex: multipotent radial glial stem/progenitor cells (RGCs) in the ventricular zone (VZ) and derived intermediate neurogenic progenitors (INPs) in the subventricular zone (SVZ).[1–3] INPs divide 1–2 times and only give rise to neurons, with regulation of their number proposed to contribute to cortical expansion.[1–6] Molecularly, a sequence of key transcription factors, Pax6->Ngn2->Tbr2->NeuroD1->Tbr1, promotes cortical neurogenesis.[7] Among these, Ngn2 is required for transition from early Pax6$^+$ radial glia to Tbr2$^+$ INPs, as well as for expansion of INPs, whereas NeuroD1 is expressed in INPs and early-differentiating neurons.[7,8] How their sequential timed expression is regulated to promote the development of normal-sized cortices is unknown.

The development of human microcephaly likely results from abnormal cortical precursor behavior. Interestingly, deletion of the distal end of human chromosome-1q is linked to microcephaly with agenesis of the corpus callosum (e.g. 9–11), and a critical region contains only a handful of genes, including *RP58*.[9–12] *RP58*, also known as *ZNF238*,[13] encodes a transcription factor with a BTB/POZ and four zinc-finger domains[14] that is highly conserved (>95%) between humans and mice, suggesting conserved functions.

Previous work has shown that *RP58* is expressed in mouse brain precursors and neurons,[15] and that its complete loss leads to defects in cortical and hippocampal development.[16] Critically, perinatal death of conventional knockout (KO) mice[16] precludes analyses in postnatal stages. Furthermore, the reported defects in cell-cycle exit, and in Pax6$^+$ and Tbr2$^+$ populations, were deduced from analyses at late corticogenesis stages after embryonic day (E) 16.5, precluding any conclusions on early defects and not providing potential molecular mechanisms for RP58 function during neurogenesis. Therefore, how RP58 acts is unknown.

We have created neural-specific *RP58* KOs and find that loss of *RP58* in the CNS leads to severe disruption of neurogenesis, resulting in a striking postnatal small-brain phenotype. Our data suggest that RP58 regulates, at early corticogenesis stages, the fate and differentiation of cortical cells, thus allowing normal brain growth. Importantly, we find that RP58 directly represses the levels of key neurogenic genes in differentiating cells. We propose that RP58 modulates stepwise the neurogenic pathway, thus contributing to the determination of the number of differentiated neurons appropriate for a given species.

## Results

**Neural-specific deletion of *RP58* causes a novel postnatal small-brain phenotype.** To address the function of RP58 specifically in the murine CNS, we generated a conditional *RP58* loss-of-function allele. The floxed *RP58* gene (*RP58$^{fl/fl}$*) was deleted in bigenic mice carrying a *Nestin*-Cre transgene[17] (Supplementary Figure 1), which drives the expression of Cre recombinase in neural precursors. Ubiquitous loss of *RP58* (hereafter *RP58* KO) produced late embryonic/early postnatal lethality, whereas neural loss of *RP58* (hereafter *RP58* cKO (conditional KO)) resulted in death at ~3 weeks. The

[1]The Wistar Institute, 3601 Spruce Street, Philadelphia, PA 19104, USA
*Corresponding author: N Dahmane, The Wistar Institute, 3601 Spruce Street, Philadelphia, PA 19104, USA. Tel: +215 495 6840; Fax: +215 495 6848; E-mail: ndahmane@wistar.org
**Keywords:** RP58; ZNF238; BTB/POZ; neurogenic progenitors; cerebral cortex; microcephaly
**Abbreviations:** RGC, radial glial stem/progenitor cell; INP, intermediate neurogenic progenitor; VZ, ventricular zone; SVZ, subventricular zone; KO, knockout; cKO, conditional knockout; ChIP, chromatin immunoprecipitation; PFA, paraformaldehyde; PBST, PBS–Triton 0.1%; FACS, fluorescence-activated cell sorting
Received 20.5.11; revised 13.9.11; accepted 16.9.11; Edited by L Greene; published online 18.11.11

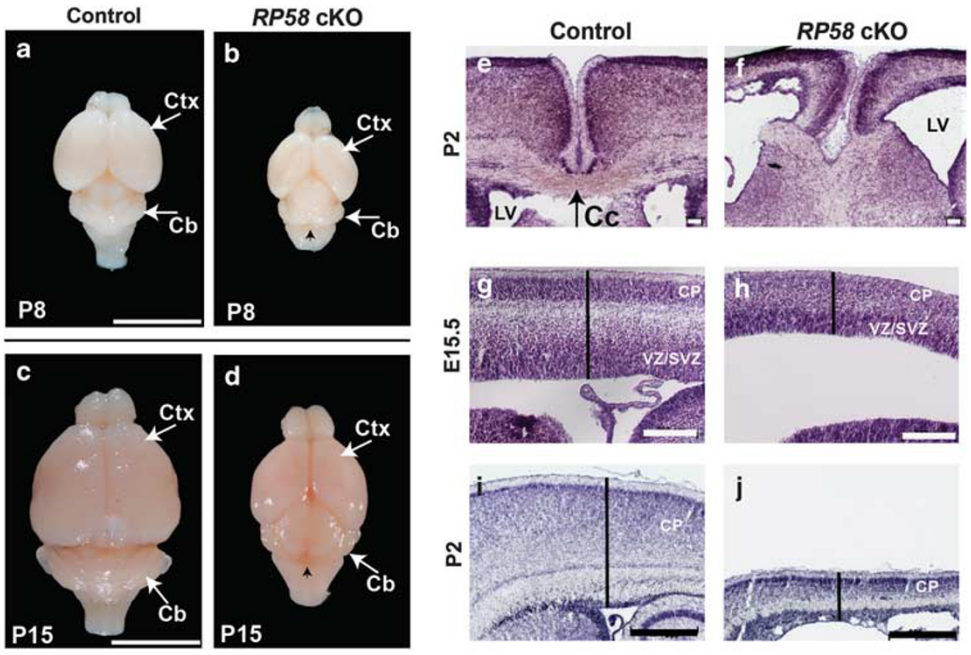


**Figure 1** Loss of *RP58* produces a novel postnatal microencephalic phenotype with a thin neocortex and absence of corpus callosum. (**a**–**d**) Dorsal views at the same magnification of control (**a** and **c**) and *RP58* cKO (**b** and **d**) brains at postnatal (P) day 8 and 15. Note the reduced size of the cerebral (ctx) and cerebellar (cb) cortices in mutant brains. The black arrows indicate the cerebellar vermis, which is lost in *RP58* mutants. (**e**–**j**) Histological analyses of control (**e**, **g** and **i**) and *RP58* mutant (**f**, **h** and **j**) cortices at E15.5 and P2 after Nissl staining, seen in a coronal section (**e** and **f**) and sagittal sections (**g**–**j**) near the midline. Mutant cortices lack a midline-crossing corpus callosum (Cc, arrows in panel **e**) and have a thin cerebral cortex as compared with the controls (**g**–**j**). Scale bars = 0.5 cm: panels **a**–**d**; 100 $\mu$m: panels **e** and **f**; 200 $\mu$m: panels **g** and **h**; 500 $\mu$m: panels **i** and **j**

cKO (*RP58*$^{fl/fl}$;*Nestin-Cre or RP58*$^{fl/-}$;*Nestin-Cre*; see Supplementary Figure 1) and control mouse littermates at P0–P8 showed no obvious differences in body size (not shown). After 2 weeks, however, a general deficit was evident, with *RP58* cKOs dying at about 3 weeks of age.

*RP58* cKO brains showed a striking reduction in brain size with a drastic decrease in cerebral and cerebellar cortical size as compared with control littermates (Figures 1a–d). Histological examination at P2 revealed a small and disorganized cortex, an enlarged ventricle and absence of corpus callosum (Figures 1e and f). Cortical thickness in the *RP58* cKO was progressively reduced starting at E15.5 and was less than half of that of the control cortex at ~P2 (Figures 1g–j and Supplementary Figure 2). Thus, analyses of our cKO mutant extend previous findings with a straight KO,[16] and highlight the requirement of RP58 for normal postnatal brain growth. Critically, loss of *RP58* in the CNS leads to a novel postnatal small-brain phenotype with loss of corpus callosum and cerebellar vermis hypoplasia, which resembles the human microencephaly phenotype linked to loss of chromosome-1qter.[9–12]

**Defective organization of the cerebral cortex in *RP58* mutants.** In order to confirm and extend the reported localization of *RP58* in the mouse brain[15] and to interpret correctly the phenotypes described above, we performed antisense RNA *in situ* hybridization analyses on sections of mouse brains at different stages of development. Expression of *RP58* mRNA in the developing cortex was highly regulated from mid-gestation to postnatal stages (Supplementary Figures 3a–d; Ohtaka Maruyama *et al*.[15]). At embryonic day (E) 10.5, *RP58* was expressed in the neural precursors near the ventricle of the dorsal telencephalon (Supplementary Figure 3a). This pattern evolved, and expression became prominent in differentiated cells of the cortical plate from E12.5 to E14.5 (Supplementary Figures 3b and c), with the intermediate zone showing high *RP58* expression transiently at E15.5 (Supplementary Figure 3d). At postnatal stages, differentiated cells in the cortical plate, comprising mostly post-mitotic neurons, showed high *RP58* mRNA levels, whereas low levels were maintained in precursors close to the ventricle[15] (Ohtaka Maruyama *et al*.[15] and data not shown).

The archetypal layered organization of the adult mammalian neocortex is of utmost functional importance for the adult, as different layers are involved in different tasks.[18] Layer-specific cortical neurons express distinctive markers[18] and are born in a precise temporal succession from cycling precursors close to the ventricle. This behavior allows them to be traced and identified by markers and birth-dating analyses.[19] The expression of the layer-specific markers *ER81*, *RORb* and *cux2* (reviewed in Molyneaux *et al*.[18]) in the control and the *RP58* cKO confirmed the thinning of the cortical plate and revealed loss of *ER81*$^+$ layer V, *RORb*$^+$ layer IV and *cux2*$^+$ layers II–IV (Figure 2a and Supplementary Figure 4). Loss of layer V neurons was also observed with *S100A10* labeling (not shown). Whereas CTIP2$^+$ layer V–VI neurons were still detectable, they failed to distribute in a gradient at the right position (Figure 2a and Supplementary Figure 5). By contrast, SATB2$^+$ layer II–IV neurons were lost or highly reduced in the *RP58* cKO (Figure 2a). These results are consistent with previous findings[16] and suggest that *RP58*

is required for proper production of cortical neurons from radial glial/stem cells and/or INPs over a protracted period.

The reduced cortical thickness of *RP58* mutants could also be due to increased apoptosis. No increase in the number of cells with cleaved Caspase-3 was detected at E14.5 (not shown) in control *versus* cKO cortices. However, *RP58* cKO cortices showed a clear increase at E16.5 ($\sim$8-fold), E18.5 ($\sim$10-fold, not shown) and P2 ($\sim$3.5-fold) (Supplementary Figure 6). This increase in cell death was also evident by western blot analysis at E18.5 (Supplementary Figure 8b). This suggests that, whereas apoptosis is not an early response to loss of *RP58*, it partly contributes to the thinning of the neocortex before death.

Analyses of the spatial distribution of neurons born at different stages during corticogenesis using BrdU birth-dating revealed a widespread deficit in neuronal positioning during cortical plate formation in *RP58* cKO brains (Supplementary Figures 7a–i).

One possible cause of the abnormal architecture of the cortical plate was suggested by the positioning of BrdU$^+$ cells labeled at E11.5 and analyzed at E15.5 (Supplementary Figures 7j–m): the normal positioning of E11.5-born cells in the marginal zone and the sub-plate of control brains was absent, and a number of labeled cells were instead found near the pial surface of cKO cortices. Moreover, analyses of CSPG$^+$ and Tbr1$^+$ cells[20] confirmed the disorganization of these cell populations and the absence of a pre-plate splitting (Supplementary Figures 7n–q), which may contribute to the positioning defect observed in the mutant.

**Inhibited neurogenesis, increased gliogenesis and persistence of early precursors in *RP58* mutant cortices.** Given that multiple types of neurons are defective in the disorganized *RP58* mutant cortex, we investigated whether the mutant could show a general deficit in neurogenic differentiation, which normally peaks between E11.5 and E17.5,[18] in favor of gliogenic differentiation, which normally peaks after E18, by testing neuronal and glial markers. Analyses at E14.5 revealed a decrease of the pan-neuronal MAP2 labeling in cKO *versus* control cortices (Figure 2b and Supplementary Figure 8a), which was confirmed by a reduction in the number of E14.5 MAP2$^+$ cells acutely dissociated from *RP58* cKO cortices (Figure 2d). Furthermore, NeuN staining at P2 and P8 indicated that the number of post-mitotic neurons present at these postnatal stages is highly reduced in the *RP58* cKO *versus* the control cortices (Figure 2b and Supplementary Figure 8c). Deficient neuronal development was also confirmed by Neurofilament M staining, which revealed reduced levels and disorganization of the expressing neurons (not shown), raising the possibility of defects in neuronal maturation in the mis-patterned mutant cortex (see above). In contrast to defective neuronal production, an increase in GFAP, a marker of astrocytes and progenitor cells, was detectable in the cortical plate and the ventricular zone at P2 (Figures 2c and e). Nestin expression characteristic of neural precursors also showed an increase in *RP58* cKO *versus* control cortices at P2 (Figures 2c and e, and Supplementary Figure 8b).

To discern the cellular and molecular basis of these cell differentiation defects, we tested for the expression of a cohort of cortical progenitor markers in the *RP58* cKO brain as compared with the controls. These analyses were performed at mid-corticogenesis (E14.5) in order to pinpoint the early events controlled by RP58 that lead to the postnatal small brain. Quantitative RT-PCR was performed on dissected medial cortices using two markers for RGCs (*blbp* and *glast*) (e.g. 21,22) and five markers for INPs (*tbr2*, *cux2*, *svet1*, *satb2* and *math2*) (e.g. 2,3,22,23). The expression of RGC markers was consistently increased $\sim$2-fold, whereas the expression of INP markers was consistently reduced $\sim$1.5- to 3-fold (Figure 2f). This coherent downregulation of INP markers was confirmed by *in situ* hybridization on cortical sections using *tbr2* and *cux2* probes at E14.5 and E16.5, respectively (Figure 2g, and Supplementary Figures 4m and n).

Together, these findings suggest that loss of *RP58* disrupts the development and normal expansion of neurogenic progenitors, whereas it may favor the maintenance of less committed RGCs and, at least partly, their glial differentiation. In support of this idea, a consistent and significant decrease in the number of proliferating phospho-Histone3$^+$ cells in the SVZ (where INPs are normally found and where they expand) was observed in E16.5 *RP58* cKO cortices as compared with control siblings (Supplementary Figure 9).

To determine whether the progenitor cells fail to become neurons and may instead choose the glial fate, we examined at P2 the fate of cells born at E16.5. After a BrdU pulse at E16.5, cortices were collected and analyzed for GFAP$^+$/

**Figure 2** Loss of *RP58* impairs normal neurogenesis. (**a**) Top: Sagittal sections of E18.5 cortices were stained with Nissl (top row) or subjected to *in situ* hybridization for the probes indicated on the left. Note the decrease of markers expressed in layer V, IV and II–IV in the *RP58* cKO (compare with Supplementary Figure 4 for the *RP58* KO). The asterisks show ectopic *ER81* expression in the VZ and residual faint *cux2* expression in the cortical upper layers. Scale bar = 100 $\mu$m. Bottom: Sagittal sections of control and *RP58* cKO E18.5 cortices showing altered localization of CTIP2$^+$ cells and strong reduction of SATB2$^+$ cells in the mutant cortices. Nuclei are labeled with the Hoechst dye. Scale bar = 200 $\mu$m. (**b**) Top: Analyses of neuronal-specific MAP2 labeling in control and *RP58* mutant cortices at E14.5. Note loss of neurons in the mutant cortices. Scale bar = 100 $\mu$m. Bottom: Sagittal sections of control and *RP58* cKO P8 cortices showing reduction in thickness and loss of NeuN-expressing neurons in the mutant brain. Scale bar = 200 $\mu$m. (**c**) Analyses of the density and morphology of Nestin$^+$ and GFAP$^+$ labeled cells by confocal microscopy in P2 control and *RP58* mutant cortices focusing on the subventricular zone (SVZ) and cortical plate (CP). Scale bar = 30 $\mu$m. (**d**) Analysis of the number of MAP2$^+$ cells in E14.5 acutely dissociated cortices. After dissociation, cells were plated 2 h before fixation and immunostaining. The number of MAP2$^+$ cells at E14.5 is reduced in the *RP58* mutant cerebral cortex when compared with the control cortex. The experiment was performed on three independent litters. The asterisk denotes significant change ($P<0.01$). (**e**) Western blot analysis of the levels of cell type-specific markers in P0 control and *RP58* mutant cortices. RP58 expression is lost in the mutants, which have increased Nestin and GFAP levels, and decreased MAP2 levels. Tubulin is shown as a loading control. (**f**) Quantification of the expression levels of multiple markers of radial glial cells (*glast, blbp*) and of intermediate neurogenic progenitors (INPs) (*svet1, math2, satb2, cux2* and *tbr2*) in cortical cells at E14.5. Analyses were performed by quantitative RT-PCR and values were normalized to the expression of the housekeeping gene *gapdh*. (**g**) Localization of the changes in the expression of *RP58* (top row) and *tbr2* (bottom row) mRNAs in E14.5 control and mutant cortices by *in situ* hybridization. Note that *tbr2* is expressed in cells in the VZ (asterisk) as well as in the SVZ (arrow). Scale bar = 100 $\mu$m

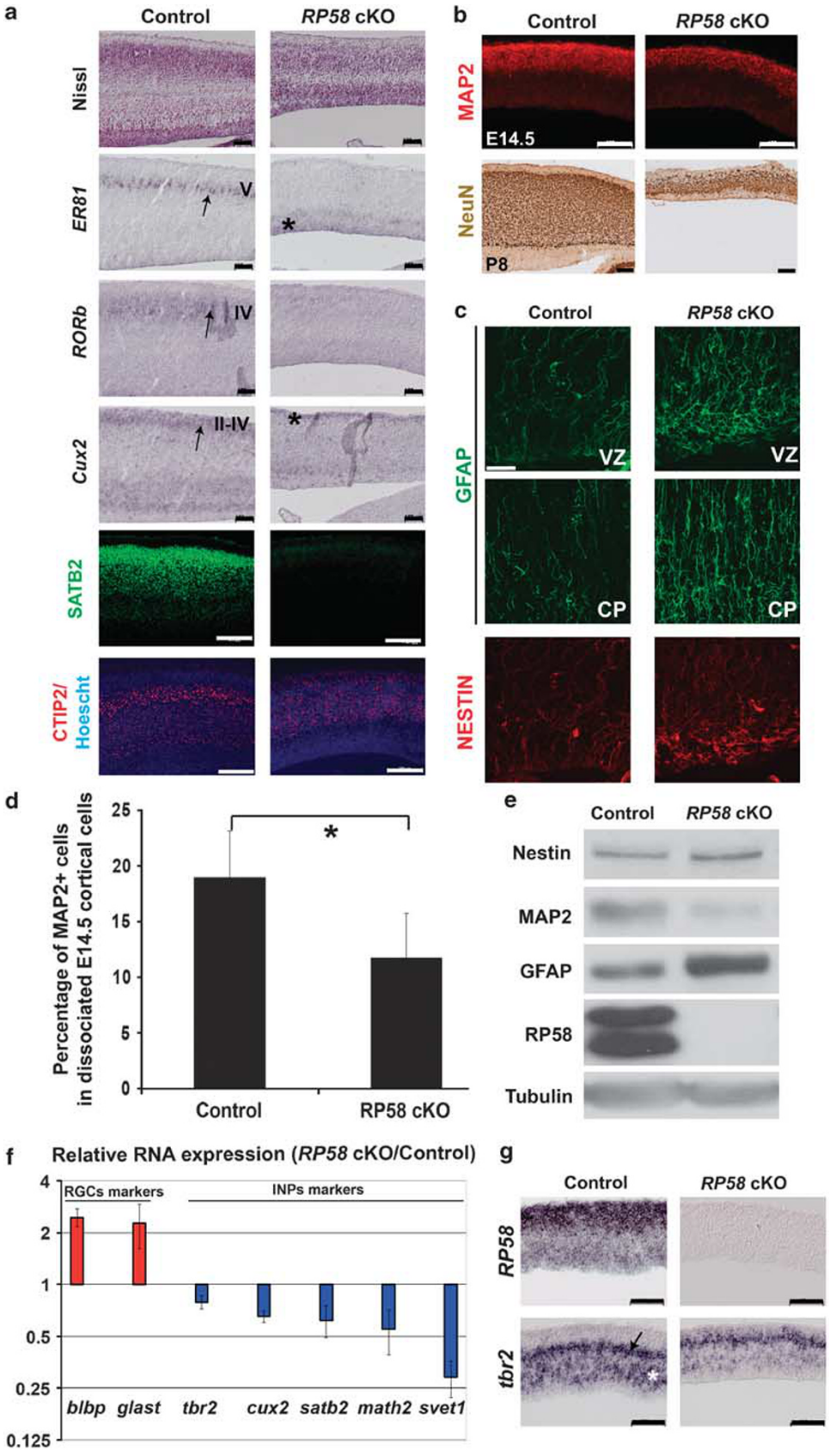
a
Control
RP58 cKO
Nissl
ER81
V
*
RORb
IV
Cux2
II-IV
*
SATB2
CTIP2/
Hoescht
b
Control
RP58 cKO
MAP2
E14.5
NeuN
P8
c
Control
RP58 cKO
GFAP
VZ
VZ
CP
CP
NESTIN
d
Percentage of MAP2+ cells
in dissociated E14.5 cortical cells
25
20
15
10
5
0
*
Control
RP58 cKO
e
Control
RP58 cKO
Nestin
MAP2
GFAP
RP58
Tubulin
f
Relative RNA expression (RP58 cKO/Control)
4
2
1
0.5
0.25
0.125
RGCs markers
INPs markers
blbp
glast
tbr2
cux2
satb2
math2
svet1
g
Control
RP58 cKO
RP58
tbr2
*

BrdU$^+$ cells: a significant increase of GFAP$^+$/BrdU$^+$ cells was observed in the *RP58* cKO as compared with the controls (Figure 3a). The results indicate that, after *RP58* deletion in the cerebral cortex, there is an increase in astrocyte production at early gliogenesis.

To investigate further whether loss of *RP58* affects the balance of neuronal and glial differentiation, we used the neurosphere differentiation assay. Primary neurosphere cultures were established from E14.5 control or *RP58* KO cortices. After primary neurosphere dissociation and growth factor withdrawal, cells were assayed for differentiation into neuronal or glial cells using neuronal or astrocytic markers. Analyses of the percentage of Tuj1$^+$ neurons and GFAP$^+$ astrocytes showed a decrease of neuronal differentiation whereas glial differentiation increased (Figure 3b). These results suggest a critical role for RP58 in preserving the balance of differentiation between the neuronal and glial lineages during embryonic development.

**Loss of RP58 causes coherent and inappropriately persistent expression of neurogenic genes.** To analyze the expression of key proneurogenic genes at different stages of neurogenesis, we developed a novel protocol for analysis of different cortical subpopulations in the presence or absence of RP58. In order to isolate cells from E14.5 control and *RP58* KO cortices by FACS, we used *tbr2::EGFP* transgenic mice, where EGFP expression is controlled by *tbr2* regulatory regions.[24] E14.5 mice were chosen to monitor early changes before manifestation of secondary effects (for instance, due to increased cell death). In these mice, EGFP expression is detected at high levels in the Tbr2$^+$ INP population but also in post-mitotic neurons owing to high EGFP protein stability.[25] In addition, we used the cell-surface marker CD133$^+$ (Prominin1$^+$) to co-label and isolate cells by FACS, as CD133$^+$ cells represent neuronal precursors and radial glial stem cells.[26] Three major subpopulations of cortical cells were identified by FACS analyses based on EGFP (and thus *tbr2*) expression and CD133 marker (Figures 4a and b): CD133$^+$;EGFP$^-$ RGC stem cells expressing high levels of *blbp*, *glast* and *pax6* (the A population); CD133$^+$;EGFP$^+$ INP cells expressing high *tbr2* (the B population); and CD133$^-$;EGFP$^+$ post-mitotic cells expressing high *tbr1* and *MAP2*, which prominently include differentiating and differentiated neurons (the C population).

As controls, we found that *RP58* was lost in mutant cells and that its expression increased as neurons differentiated from RGCs to INPs and to post-mitotic maturing neurons (Figure 5), a finding which is in perfect agreement with *in situ* hybridization results (Supplementary Figure 3). Analyses of the expression of these markers in cells sorted from the mutant indicated similar profiles as in the controls, suggesting that the A, B and C pools in *RP58* KO are comparable to their normal counterparts in terms of basic major cell identity (Supplementary Figure 10). *RP58* KO cortices had slightly

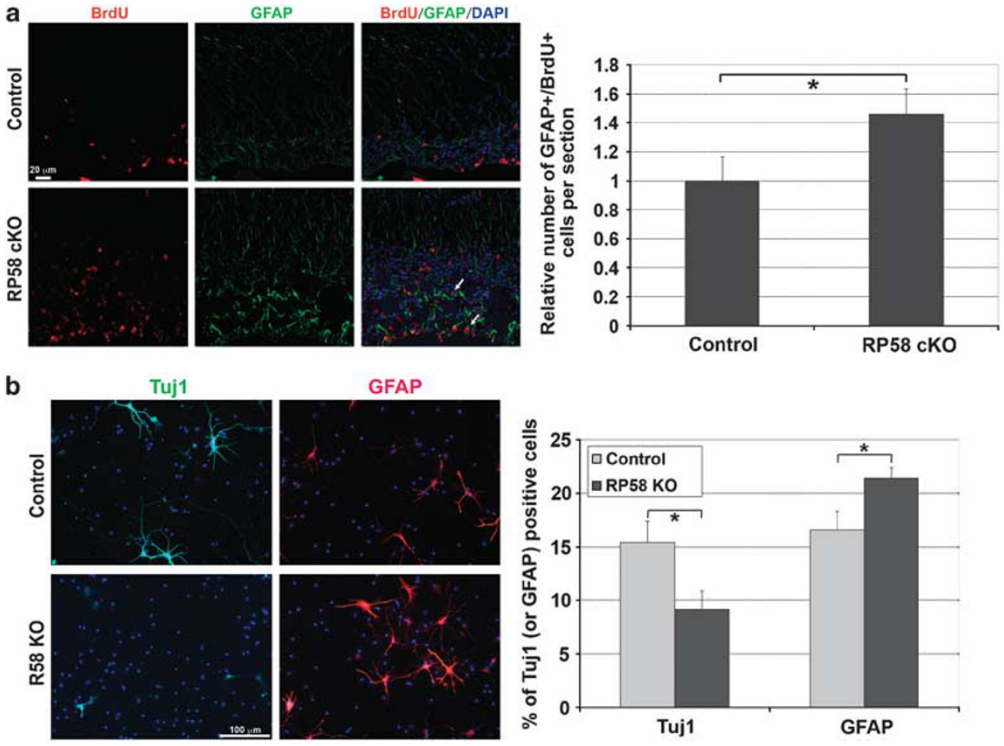


**Figure 3** Loss of RP58 leads to increased glial differentiation. (**a**) The origin of the astrocytes in the cortical VZ/SVZ was determined in BrdU birth-dating experiments: dividing cells were labeled with a BrdU pulse at E16.5 and examined for BrdU and GFAP expression at P2. BrdU$^+$/GFAP$^+$ cell counting was performed on sections from three different brains for each genotype and indicated that more astrocytes were produced at E16.5 in the RP58 mutant mice as compared with the control cortex. The asterisk denotes significant change ($P<0.05$). Scale bar = 20 $\mu$m. (**b**) E14.5 cerebral cortices were dissociated and grown as primary spheres at clonal density. Primary spheres were then dissociated and differentiated for 3–4 days. The number of neurons (Tuj1$^+$ cells) and astrocytes (GFAP$^+$ cells) was counted for each differentiation assay. Three independent experiments (three different litters) were analyzed. Neuronal differentiation is highly reduced in the RP58 mutant in favor of glial differentiation. The asterisk denotes significant change ($P<0.05$). Scale bar = 100 $\mu$m

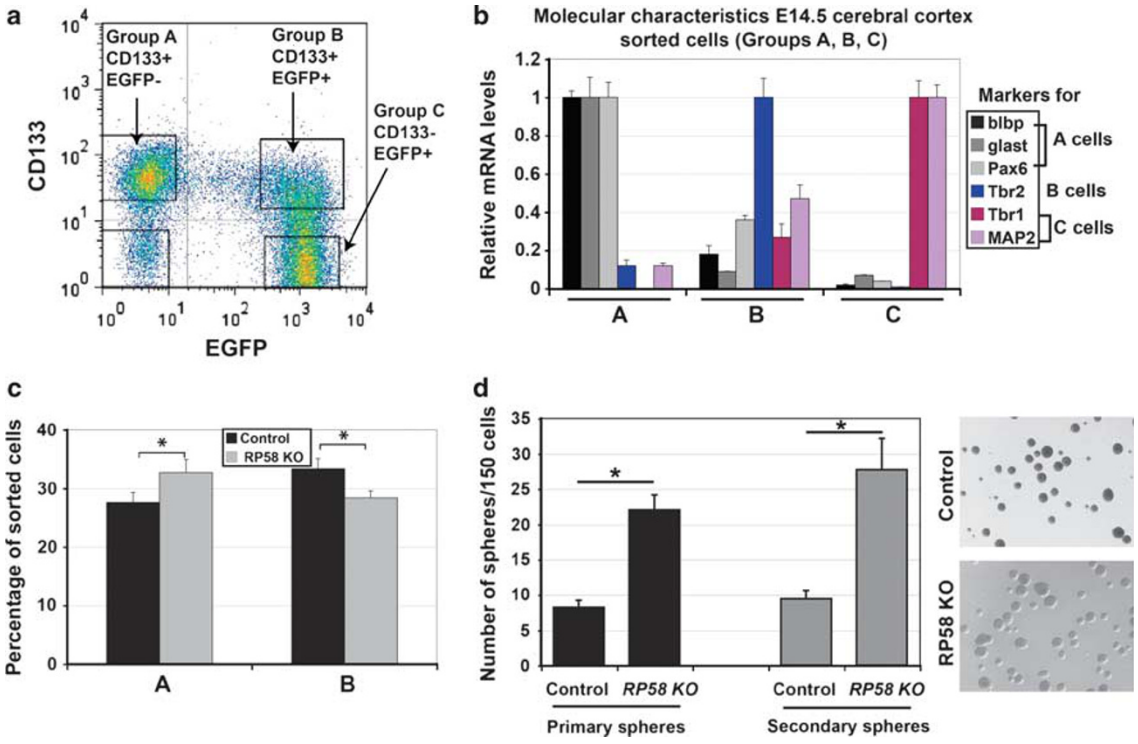


**Figure 4** Deregulation of progenitor pools was revealed by cell sorting in *RP58* mutant cortices. (**a**) FACS graph showing separation of E14.5 cortical cells depending on their expression of CD133 (Prominin1) and EGFP, the latter driven from the *tbr2* regulatory region in *tbr2: EGFP* mice. The subpopulations of cells include the following: Group-A: $CD133^{+}/EGFP^{-}$-containing RGCs in the VZ; Group-B: double positives, containing INPs in the SVZ; and Group-C: $CD133^{-}/EGFP^{+}$, containing differentiating/differentiated cortical neurons. (**b**) Characterization of the three cell populations described in panel **a** by expression of key molecular markers of RGCs (*blbp*, *glast*, *pax6*), INPs (*tbr2*) and neurons (*tbr1*, *MAP2*). (**c**) Quantification of the pool size of A and B cells in control and *RP58* KO cortices. A small increase in A cells and a slight decrease in B cells were observed in the mutant cortices at E14.5. The asterisks denote significant changes ($P<0.05$ for A cells, $P<0.01$ for B cells). (**d**) Loss of RP58 leads to an increased number of neocortical neurospheres. E14.5 cerebral cortices were dissociated and grown as primary spheres at clonal density (less than 10 cells/$\mu$l). After 7 days, primary spheres were dissociated and challenged to form secondary spheres also at clonal density. The number of primary and secondary neurospheres was assessed visually in triplicate assays for each experiment. Three independent experiments with three different litters were analyzed. A two-tailed *t*-test was applied for statistical analysis. The asterisks denote significant changes ($P<0.001$)

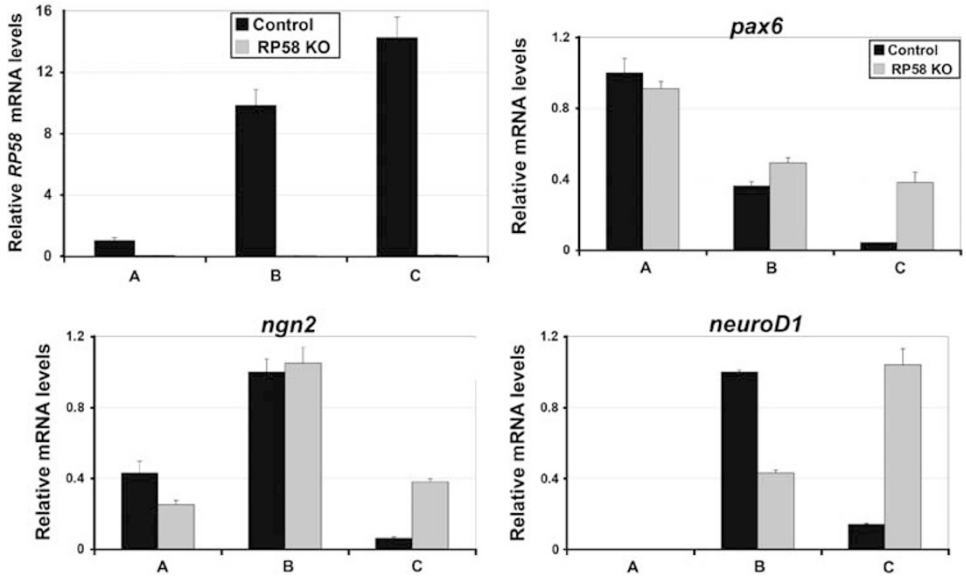


**Figure 5** Loss of RP58 leads to deregulation of proneurogenic gene expression. Analyses of the expression levels of *RP58*, and key RGC and INP regulators in sorted cell populations in control and *RP58* mutant cortices at E14.5. Note (1) loss of *RP58* expression in the mutant and (2) the consistent increase of *pax6*, *ngn2* and *neuroD1* in C cells. The diagrams are from a representative experiment. Experiments were performed in triplicates from three independent litters, with similar results

enhanced RGC and slightly decreased INP pools as compared with the controls (Figure 4c), whereas the number of cells in pool C was not greatly modified between control and *RP58* KO cortices at these early time points.

To investigate whether loss of RP58 also had an effect on the self-renewal properties of multipotent progenitors in the cerebral cortex, we established primary neurosphere cultures from E14.5 control and *RP58* KO cortical cells at clonal density. Primary neurospheres were then subjected to secondary cloning conditions to evaluate the number of stem cells derived from the primary founding stem cells in the primary neurospheres. Primary spheres from *RP58* mutant neocortex produced more secondary neurospheres than did control cells, indicating higher self-renewal capacities for *RP58* mutant neural stem cells in culture (Figure 4d). These results raise the possibility that RP58 normally acts to restrict the number of stem cells in the cerebral cortex perhaps by promoting their differentiation directly into neurons or into INPs.

Strikingly, analyses of the key proneurogenic genes *pax6*, *ngn2* and *neuroD1* showed their coherent upregulation in differentiating cells (the C population; Figure 5). Individual changes were also observed for each gene in different populations and future studies should address their cause. Nevertheless, the consistent overexpression of *pax6*, *ngn2* and *neuroD1* in C cells suggests that the expression of RGC and INP markers is inappropriately maintained in differentiating neurons, indicating that RP58 could normally repress their expression when cells begin, or for cells to begin, their differentiation, thus regulating the timing of their expression to ensure proper neurogenesis.

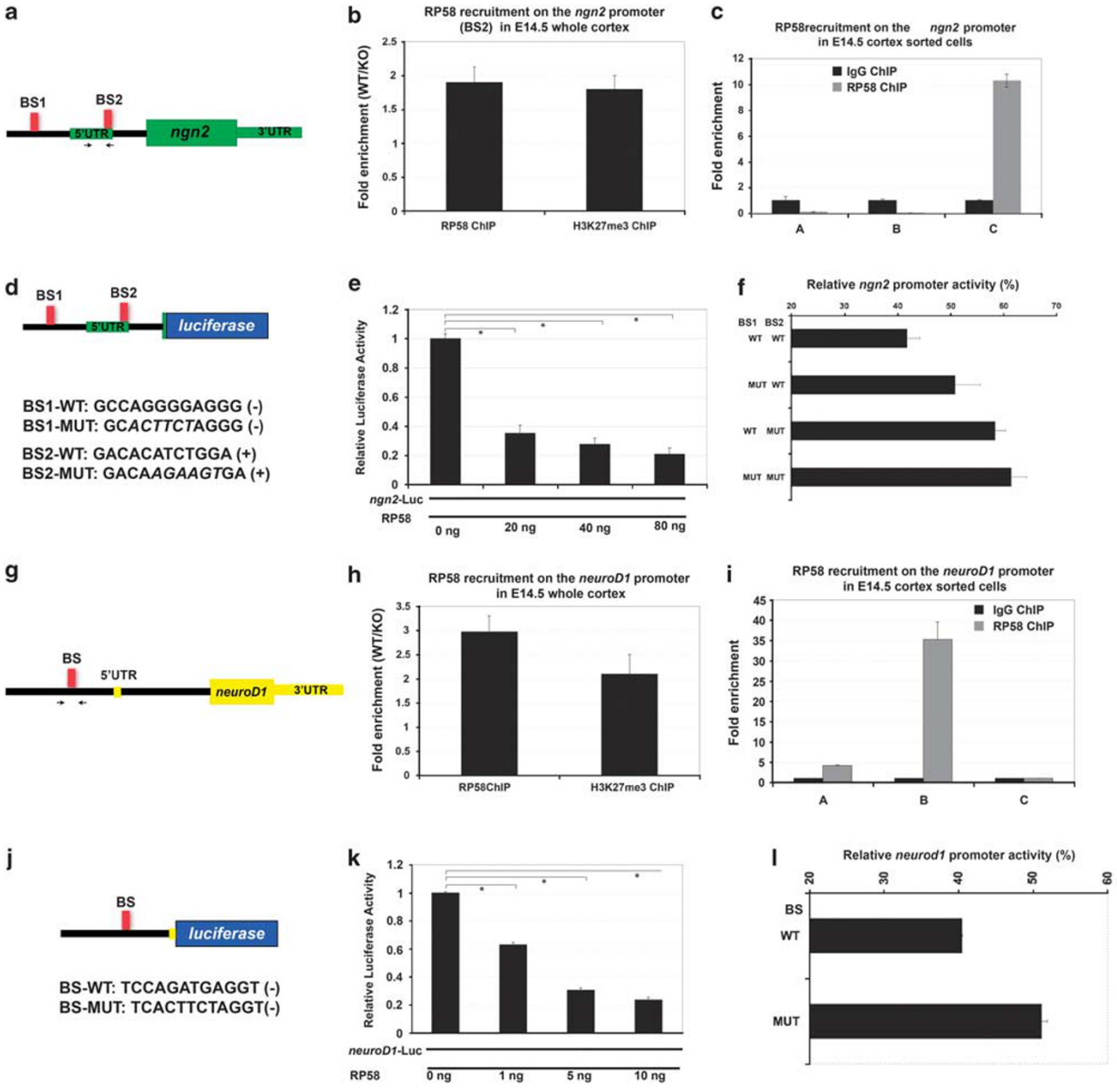

**Direct regulation of *ngn2* and *neuroD1* by RP58.** As *pax6*, *ngn2* and *neuroD1* encode essential sequential functions for neurogenesis (e.g., Hevner,[7] Hevner *et al*.[8] and Miyata *et al*.[27]), we investigated the possibility that RP58 regulates the number of neurons in the developing cerebral cortex by directly regulating these key neurogenic determinants.

Putative conserved consensus RP58-binding sites[14] were detected in the proximal regulatory regions of *ngn2* and *neuroD1* (Supplementary Figure 11). Chromatin immunoprecipitation (ChIP) analyses using an anti-RP58 antibody[13] were thus performed for these two genes first on whole cortices and then on sorted cells from control cortices taken at the same stage. In ChIP, RP58 was found to bind a specific DNA fragment containing a putative RP58-binding site within a proximal *ngn2* regulatory region (BS2, position $+295$ to $+304$ in exon-1; Figure 6a), showing an $\sim$2-fold enrichment over background obtained using the *RP58* KO tissue (which does not contain any RP58 protein and thus constitutes an ideal control for these ChIP experiments) (Figure 6b). In addition, RP58 in ChIP experiments was also found to bind a specific DNA fragment containing another putative RP58-binding site (BS1, position $-202$ to $-213$ in the 5′ untranscribed region (Figure 6a); Supplementary Figures 12a and b). Consistent with the proposed role of RP58 as a transcriptional repressor,[14] RP58 binding perfectly correlated with the presence of a repressive trimethylated histone H3K27 mark (Figure 6b). Additional control experiments using an IgG control and a genomic region with no RP58-binding site also confirmed enrichment of RP58 at the *ngn2* promoter (Supplementary Figure 13).

ChIP–PCR analyses using sorted cells from the A, B and C populations (in *tbr2::EGFP* mice as above) demonstrated a 10-fold increase in RP58 binding to an *ngn2* regulatory region over an IgG control, specifically in differentiating/differentiated control C cells (Figure 6c). We interpret these data to indicate that RP58 normally represses *ngn2* in differentiating neurons and that loss of RP58 de-represses *ngn2* expression in these cells, changing its temporal pattern of expression and thus preventing normal differentiation. *In situ* hybridization analyses confirmed a weak but consistent de-repression of *ngn2* in differentiated cells as we found an abnormal ectopic *ngn2*$^+$ domain in the cortical plate of mutant cortices at E16.5, a zone that does not express *ngn2* (Supplementary Figure 14).

To extend these findings and investigate whether regulation of *ngn2* by RP58 is functional, we performed luciferase reporter assays using the *ngn2* regulatory region containing the RP58-binding sites described above. Fusion of this promoter fragment to the *firefly luciferase* coding region (*ngn2*-Luc) resulted in luciferase expression in transfected HEK293 cells. Importantly, co-transfection of RP58 resulted in the repression of reporter activity in a dose-dependent manner (Figures 6d and e). Moreover, this repression by RP58 is dependent on its zinc-finger domains as a construct lacking them failed to repress luciferase activity driven by the *ngn2* promoter (not shown). As control, mutation of the RP58-binding sites BS1 and BS2 greatly diminished the repressive activity of RP58 on the *ngn2*-Luc reporter (Figure 6f).

Similar analyses with *neuroD1* showed the presence of a single consensus RP58-binding site in the upstream regulatory region (Figure 6g), and we were able to chromatin immunoprecipitate a genomic fragment with this site using the RP58 antibody (Figure 6h and Supplementary Figure 13). As with *ngn2*, it also correlated with a repressive H3K27me3 mark (Figure 6h). Analyses of the A, B and C cell populations sorted for CD133 and *tbr2::EGFP* as above showed recruitment of RP58 to the *neuroD1* promoter in INPs, the B population (Figure 6i). We interpret this to indicate that RP58 normally represses *neuroD1* in INPs. Finally, as with *ngn2*,

**Figure 6** RP58 directly regulates *ngn2* and *neuroD1* expression. (**a**) A schematic diagram showing the localization of two putative RP58-binding sites and the primers (arrrows) used in the ChIP–PCR in panels **b** and **c**. The *ngn2* gene is indicated in green. The putative RP58-binding sites (BS1 and BS2) in the 5′ *ngn2* genomic region are indicated by red boxes. (**b**) ChIP analyses of RP58 recruitment and presence of trimethylated histone H3K27 (H3K27me3) as a marker of repressed loci in control and *RP58* mutant cortices using primers specific to the *ngn2* genomic region encompassing the RP58-binding site BS2 at chr3:127336163 + 127336391 (see scheme in panel **a**). Note that the histograms show the fold enrichment of WT/KO. (**c**) Specific and preferential binding of RP58 to the *ngn2* genomic region in the differentiated C cell populations. This experiment was performed on cells sorted from two independent litters, with primers encompassing the same binding site BS2, with similar results. Note that the background thresholds obtained with a ChIP experiment using an isotyped IgG are set at 1 (black bars). (**d**) Top: A schematic diagram showing the *ngn2-luciferase* construct (*ngn2-luc* plasmid: *ngn2* regulatory region containing two RP58-binding sites) used for the data presented in panels **e** and **f**. Bottom: Sequences of the two RP58-binding sites, BS1 and BS2, in the *ngn2* promoter region. Mutant versions of BS1 and BS2, and their sequence orientations are noted. (**e**) Transcriptional repression of an *ngn2* regulatory region driving the expression of firefly luciferase by RP58. HEK293T cells were transfected with the *ngn2-luc* plasmid (see panel **a**). *Ngn2-luc* was transfected alone or with increasing doses of an RP58-expressing plasmid. Luciferase activity was assayed 48 h after transfection. Shown is a representative experiment of three independent biological replicates with similar results. The asterisks denote significant changes ($P<0.001$). (**f**) Mutation of RP58-binding sites impairs its repression of the *ngn2* promoter. The *ngn2-luc* constructs containing no (WT), 1 or 2 mutant (MUT) RP58-binding sites were co-transfected into HEK293T cells together with an RP58-expressing plasmid. Luciferase activity was normalized as percentage of the same reporter activity in the absence of exogenous RP58. Shown is a representative experiment of three independent biological replicates with similar results. A statistically significant difference of activity was observed between BS1-MUT and BS2-MUT ($P<0.01$), as well as between the single mutant BS1-MUT and the double mutant BS1-MUT + BS2-MUT ($P<0.01$). (**g**) A schematic diagram showing the localization of the primers (arrows) used in the ChIP–PCR in panels **h** and **i**. The *neuroD1* gene is indicated in yellow. The unique consensus RP58-binding site (BS) in the proximal 5′ *neuroD1* genomic region is indicated by a red box. (**h**) ChIP analyses of RP58 recruitment and presence of trimethylated histone H3K27 (H3K27me3) as a marker of repressed loci in control and *RP58* mutant cortices using primers specific to the *neuroD1* genomic region encompassing the RP58-binding site. Note that the histograms show the fold enrichment of WT/KO. (**i**) Specific and preferential binding of RP58 to the *neuroD1* genomic region in cells of the progenitor B cell population. Note that the background thresholds obtained with a ChIP experiment using an isotyped IgG are set at 1 (black bars). (**j**) Top: A schematic diagram showing the *neuroD1-luciferase* construct used for the data presented in panels **k** and **l**. Bottom: Sequence of the RP58-binding site BS in the *neuroD1* promoter region. The mutant version of BS and sequence orientation is noted. (**k**) Transcriptional repression by RP58 of a *neuroD1* regulatory region driving the expression of firefly luciferase. HEK293T cells were transfected with the *neuroD1-luc* plasmid (*neuroD1* regulatory region containing one RP58-binding site driving a *luciferase* reporter gene). *NeuroD1-luc* was transfected alone or with increasing doses of an RP58-expressing plasmid. Shown is a representative experiment of three independent biological replicates with similar results. The asterisks denote significant changes ($P<0.001$). (**l**) Mutation of RP58-binding site impairs its repression of the *neuroD1* promoter. The *neuroD1-luc* constructs containing the WT or mutant BS were co-transfected into HEK293T cells together with an RP58-expressing plasmid. Luciferase activity was normalized as percentage of the same reporter activity in the absence of exogenous RP58. Shown is a representative experiment of three independent biological replicates with similar results

fusion of a regulatory region containing the consensus RP58-binding site upstream from *neuroD1* to *luciferase* resulted in activity that was repressed in HEK293 cells by exogenous RP58 in a dose-dependent manner (Figures 6j and k). Mutation of the RP58-binding site impaired the reduction of luciferase activity (Figure 6l). RP58 thus directly modulates the expression of at least two key proneurogenic genes.

## Discussion

Ensuring that the correct number of neurons develops in an orderly manner is a requisite for brain growth and function. A cascade of neurogenic transcription factors, including *ngn2* and *neuroD1*, induces precursor cells to become neurons (e.g. 7,8). However, the mechanisms that regulate the timing and levels of these critical neurogenic factors remain largely unknown. Here, we studied the requirement of RP58 in this process using both ubiquitous and neural-specific mouse KOs.

We find that specific deletion of *RP58* in Nestin$^+$ CNS precursors results in a postnatal small-brain phenotype with defects in neuronal production and differentiation. Our CNS-specific conditional strategy and its finding that our cKO and control littermates are indistinguishable at birth allow us to conclude that these defects are CNS-intrinsic and not due to loss of RP58 elsewhere in the body, as may be the case for perinatal death of the total KO reported recently[16] (and this paper). The *RP58* cKO mice survive up to 3 weeks at a time when the brain is already well constructed. Starting at P2, cKO brains have a novel postnatal phenotype not observed previously in the straight KOs that die perinatally:[16] reduced neocortex (both in extent and thickness) and loss of corpus callosum.

We provide evidence for a major role of RP58 in the promotion of ordered and correctly timed neurogenesis leading to proper layer formation and cortical growth. In its absence, neuronal differentiation is abortive, layers are not formed or are defective, and progenitor cells may instead adopt glial fates. RP58 appears to control neurogenesis at multiple points as suggested by defective differentiation of multiple neuronal types in different layers over an extended period, and deregulation of *pax6*, *ngn2* and *neuroD1* gene expression. A recent paper describing the phenotype of the straight *RP58* KO showed that there is an increase of progenitor cells in the E18.5 mutant cortices.[16] However, as these analyses were performed one day before death or birth, corresponding to a time when the major neurogenic wave from the ventricular zones is over,[16] these results are not informative as to a possible role of RP58 in RGCs or INPs. It is important to note, however, that the previous report of the *RP58* KO investigated cell-cycle defects as early as E12.5, and detected defects only at E16.5. These results are in agreement with and complement our study. Our data, in addition, allow us to suggest that RP58 controls at least two major transitions in neurogenesis: (1) The development of RGCs into INPs, the expansion of which in the SVZ has been proposed to underlie the enormous increase in cortical volume during evolution and ontogeny;[2] and (2) the differentiation of INPs into mature neurons. Thus, defects in brain growth are likely due to diminished neurogenic progenitor and differentiated neuronal pools.

How does RP58 regulate neurogenesis? We find that RP58 has a direct role in the regulation of at least two key factors in the neurogenic cascade Pax6->Ngn2->Tbr2->NeuroD1->Tbr1.[7,8] We show that RP58 acts to restrict the expression of *pax6* to RGCs and *ngn2* and *neuroD1* to INPs, as, in the *RP58* mutant, these are mis-expressed in more differentiated cells, that is, their temporal repression is faulty and precursors' character is inappropriately maintained in more differentiated cells. Moreover, we show that RP58 directly regulates *ngn2* and *neuroD1* in cortical cells. We propose that repression of sequential proneurogenic genes endows RP58 with a sustained pro-neuronal differentiation function, which is consistent with its dynamic expression pattern, in the VZ, then in the SVZ and finally, and most critically, in the differentiating neurons in the cortical plate (this work,[15]). We propose that a precisely timed and measured repressive function of RP58 in subsequent neurogenic stages is essential for normal production of the correct number of cortical neurons, and thus cortical size.

Our findings in mice may have important implications for human development and disease. Deletion of a region of chromosome-1q, containing *RP58*, leads to human syndromes characterized by the presence of microcephaly and corpus callosum agenesis (e.g. 10,28), phenotypes that are remarkably similar to the postnatal phenotype of CNS-specific *RP58* loss. Whereas the common deleted region in 1qter deletion microcephaly syndrome patients is being refined, only five genes and/or referenced sequences are general candidates.[10] The conservation of *RP58* sequence and chromosomal location in mice and humans, together with our present results, allows us to suggest that *RP58* may indeed be a key gene for the development of the normal human brain and that its loss or downregulation contributes to human microencephaly. We propose that modulation of RP58 function during evolution drives crucial changes in the timing of differentiation from RGCs to INPs to neurons and results in brains and cortices of varying sizes. Changes in RP58 function may have contributed to the expansion of the human neocortex.

### Materials and Methods

**Mice crosses and genotyping.** After cross of *RP58*$^{fl/+}$ heterozygotes with a *CMV-Cre* transgenic line, *RP58*$^{+/-}$ heterozygous mice were established. *RP58*$^{+/-}$ heterozygotes were bred in order to collect *RP58*$^{-/-}$ homozygous mutants for analyses. *RP58* conditional mutants were obtained from crossing double heterozygous mice (*RP58*$^{fl/+}$; *Nestin-Cre*) with *RP58* homozygous floxed (*RP58*$^{fl/fl}$) mice.

**Histology and immunostaining.** Embryos were dissected and fixed in 4% paraformaldehyde (PFA) solution (pH7.4) in 0.1 M phosphate buffer on ice for up to 2 h or overnight. Postnatal mice were perfused using the 4% PFA solution, then post-fixed in the same solution for 1 h. After fixation both embryos and brains were rinsed in PBS, cryoprotected in 30% sucrose–PBS solution, frozen in OCT and sectioned at a thickness of 12–16 $\mu$m. Sections were stained with cresyl violet solution or processed for immunostaining. For immunostaining, sections were rinsed in PBS–Triton 0.1% (PBST) and then incubated up to 1 h in PBST with 10% heat-inactivated goat serum. Incubation with an appropriate primary antibody solution was performed overnight at 4 °C. Sections were then rinsed twice in PBST and incubated for 1 h at room temperature with a secondary antibody, washed in PBST and mounted in mounting media. The following primary and secondary antibodies were used: mouse anti-BrdU (1/200; Becton Dickinson, San Jose, CA,

USA, 347580), rabbit anti-cleaved caspase-3 (1/400; Cell Signaling, Danvers, MA, USA, 9661), rat anti-GFAP (gift from Judith Grinspan, Children's Hospital of Philadelphia), mouse anti-MAP2 (1/6000; Sigma, St. Louis, MO, USA, M4403), mouse anti-Nestin (1/600; Chemicon, Billerica, MA, USA, MAB353), rabbit anti-Neurofilament M (1/200; Millipore, Billerica, MA, USA, AB1987), mouse anti-CSPG (1/200; Sigma, C8035, clone CS-56), rabbit anti-PH3 (1/200; Upstate, Billerica, MA, USA, 06–570), rabbit anti-Tbr1 (1/1000; Millipore, AB9616), rat anti-CTIP2 (1/200; Abcam, Cambridge, MA, USA, 18465), mouse anti-SATB2 (1/50; Abcam, 21502) and mouse anti-NeuN (Chemicon, MAB377). Adequate fluorophore-conjugated or biotinylated secondary antibodies were used to label the primary antibodies. Characterization of the RP58 antibody has already been described.[13]

***In situ* hybridization.** *In situ* hybridization on sections was performed as described using digoxigenin (DIG)-labeled RNA probes.[29] DIG-labeled antisense riboprobes were generated from linearized plasmids encoding *cux2*,[30] *ER81* (EST BG974260), *ngn2*,[31] *reelin* (http://www.stjudebgem.org; NM_011261), *Rorβ*,[30] *tbr1* (PCR fragment nt 2419–2927; NM_009322), *tbr2*,[32] *CTGF*[33] and *RP58*.[13]

**Western blotting.** Protein lysates were prepared from frozen tissues in RIPA buffer (HEPES 50 mM (pH7.4), sodium deoxycholate 0.5%, NaCl 150 mM, NP-40 1%, SDS 0.1%). A 100- (for E18.5–P0 cortices) or 35-$\mu$g (for E14.5 cortices) weight of proteins was loaded on an SDS-PAGE gel and transferred onto PVDF membranes (Millipore). The membranes were then incubated with the following antibodies: anti-RP58, anti-Nestin (Chemicon, MAB353), anti-MAP2 (Sigma, M4403, clone HM-2), anti-GFAP (Sigma, G3893, clone G-A-5), anti-cleaved caspase-3 (Cell Signaling, 9661) and anti-tubulin (Sigma, T5168, clone B-5-1-2).

**E14.5 cortical dissociated cells.** Acutely dissociated cortical cells were obtained and cultured for 2 h as described.[21] Cells were then fixed and stained with MAP2 antibodies.

**Cortical cell sorting.** *RP58*$^{+/-}$ mice were crossed with transgenic mice expressing EGFP under *tbr2* regulatory sequences.[24] *tbr2::EGFP* mice (GENSAT project) were obtained from the MMRRC (Mutant Mouse Regional Resource Center). E14.5 cerebral cortices from *tbr2::EGFP* embryos were dissociated as described previously.[21] Dissociated cortical cells were resuspended in PBS, incubated with phycoerythrin-conjugated CD133 antibodies (Miltenyi, Auburn, CA, USA, 1 : 50) for 30 min on ice, washed with cold PBS and then sorted in cold PBS.[26] FACS was performed using a Becton Dickinson FACS-Aria. Total RNA was isolated from sorted cells using the RNeasy plus mini kit (Qiagen, Valencia, CA, USA) and reverse-transcribed into cDNAs.

**Neurosphere formation assay and differentiation assay.** E14.5dpc cortices were dissected in cold HBSS and fractioned in small pieces with a scalpel. The cortical pieces were then digested in a trypsin 0.05%–EDTA solution for 15 min at 37 °C. After trypsin inactivation, the tissues were mechanically dissociated through a fire-polished and FBS-coated Pasteur pipette. The homogenate was centrifuged for 5 min and resuspended in neurosphere culture media (DMEM/F12 (Gibco, Carlsbad, CA, USA, 11330), B27 (Gibco, 1 ×), N2 (Gibco, 1 ×), glutamine (Cellgro, Manassas, VA, USA, 2 mM) and penicillin (50 U/ml)/streptomycin (50 $\mu$g/ml), FGF (10 ng/ml), EGF (10 ng/ml)). Dissociated cells were seeded in a flask to form primary neurospheres at a clonal density. For the self-renewal assay, primary neurospheres were then collected and mechanically dissociated into single cells. These single cells were seeded again to form secondary neurospheres at a clonal density. Both primary and secondary neurospheres were counted after 7 days growth. For the differentiation assay, dissociated single cells from primary neurospheres were rinsed in neurosphere media without growth factors and plated onto poly-D-lysine coverslips at a density of 200 000 cells per well in 24-well plates without growth factors. After 3–4 days in the differentiation media, cells were fixed with 10% PFA solution for 10 min and processed for immunocytochemistry, as described above, using rat anti-GFAP and mouse anti-$\beta$-tubulin-III (Tuj1, 1/1000; Covance, Emeryville, CA, USA, MMS-435P) antibodies. FITC-conjugated anti-rat and anti-mouse secondary antibodies (Vector Lab, Burlingame, CA, USA) were used. Also, nuclei were counterstained with Hoechst (Sigma). GFAP- and Tuj1-positive cells were counted with a fluorescence microscope using a × 20 objective (Axioskop; Zeiss, Thornwood, NY, USA). At least five independent fields for each culture condition were counted. The analysis was performed on three independent litters (each containing representative genotypes). Statistical analysis was performed by Student's *t*-test.

**Quantitative RT-PCR.** Total RNA was extracted from whole E14.5 cortices using the TRIzol reagent (Invitrogen, Carlsbad, CA, USA), or from sorted cells using the RNeasy plus mini kit (Qiagen), and reverse-transcribed into cDNAs. Superscript reverse transcriptase-II (Invitrogen) was used for cDNA synthesis (2 $\mu$g of total RNA for whole cortices, 0.4 $\mu$g for sorted cells). Real-time PCR was performed with a SYBR Green probe using an ABI Prism 7000 according to the manufacturer-specified parameters. Each sample was run in triplicate and the RNA level for each gene was normalized to the expression of the housekeeping gene *gapdh*. Gene expression was assessed in at least three mutant and three control cortices from three different litters. The primers used for amplification are available upon request.

**Quantitative ChIP–PCR.** Cross-linked chromatin from E14.5 WT and *RP58* KO cortices was prepared according to Lee *et al*.[34] Briefly, tissues were treated with 1% formaldehyde solution for 10 min to capture the DNA–protein interactions, homogenized and cross-linked cells were collected by centrifugation. The cells were lysed and sonicated to generate bulk chromatin, which contained DNA fragments that varied in size from 200 to 400 bp. Solubilized chromatin was immunoprecipitated using specific antibodies (anti-RP58, anti-H3K27trimethyl (Abcam)) in the presence of pre-blocked 50 $\mu$l of Dynal protein-G beads (Invitrogen) at 4 °C for 16 h. Bound nucleoprotein complexes were extensively washed and the retained DNA–protein complexes were eluted before the cross-linking was reversed. The ChIP-enriched DNA was purified and specific primers were used to amplify the promoter sequence of *ngn2* or *neuroD1* by SYBR Green-based real-time PCR. Fold enrichment of *ngn2* or *neuroD1* regulatory sequence was calculated relative to the *RP58* KO mice using the $2_{\mathrm{T}}^{-\Delta\Delta C}$ method. A similar procedure was used for E14.5 cerebral cortex sorted cells.

The sequences of the primers used to amplify the *ngn2* genomic region encompassing a RP58 potential binding site BS1 are as follows (5′ to 3′): Forward primer: ccaacaggagctttagaaccat; reverse primer: ctccccagcttattcttttcat. These primers amplify the mouse genomic region chr3:127335761−127335928 (168 bp). The sequences of the primers used to amplify the *ngn2* genomic region encompassing another RP58 potential binding site BS2 are as follows (5′ to 3′): Forward primer: cgagaacgacaacacacga; reverse primer: cggcatgcacacttacctac. These primers amplify the mouse genomic region chr3:127336163-127336391 (229 bp).

The sequences of the primers used to amplify the *neuroD1* genomic region encompassing a RP58 potential binding site are as follows (5′ to 3′): Forward primer: GAGCAGGTGACCGTTAGGTT; reverse primer: GGTGG CTGGCTTCTAATCTC. These primers amplify the mouse genomic region chr2:79297481−79297666 (186 bp).

**Wild-type and mutant *ngn2* and *neuroD1* reporter constructs.** A putative *ngn2* promoter region (1127 bp) containing two RP58 potential binding sites[14] was cloned from mouse genomic DNA using the two primers as shown in Figure 4d (forward primer: CCCCTAATGAGCTGCTGAAAGG and reverse primer: ATCCTGAGAAAGAAGAGGCAGATG). The fragment was inserted into a pGL3-basic vector (Promega, Madison, WI, USA), which encodes a firefly luciferase reporter.

The sequences, CCCCTG in BS1 and CATCTG in BS2, were mutated to AGAAGT using the QuikChange Site-Directed Mutagenesis Kit (Stratagene, Santa Clara, CA, USA). The mutant constructs used in our study carry the endogenous *ngn2* promoter with either one or two of the RP58-binding sites mutated. Each mutation was confirmed by sequencing.

A putative *neuroD1* promoter region (1663 bp) containing one RP58 potential binding site[14] was cloned from mouse genomic DNA using the two primers as shown in Figure 4j (forward primer: CCACAATGCCTTGCTTTTC and reverse primer: GGACACCTTGCCTTCTGC). The fragment was inserted into the pGL3-basic vector. In the mutant construct, CATCTG on the binding site was mutated to AGAAGT.

**Luciferase assays.** HEK293T cells were seeded in 24-well plates in DMEM containing 10% FBS, 2 mM L-glutamine and penicillin (50 U/ml)/streptomycin (50 $\mu$g/ml), and transfected with a total of 250 ng of DNA including *ngn2*-Luc (100 ng, WT or mutant) and a *Renilla* luciferase construct (25 ng; Promega) with or without increasing doses of an RP58-expressing plasmid (0, 20, 40 or 80 ng). Cell extracts were prepared 48 h after transfection and luciferase activity was measured using the Dual-Luciferase Reporter Assay System (Promega). Three independent experiments were analyzed, each of them being performed in triplicate. A similar approach was used to test *neuroD1*-Luc activity.

### Conflict of Interest

The authors declare no conflict of interest.

**Acknowledgements**. We thank Frank Rauscher, Ariel Ruiz i Altaba, Louise Showe, Michael Showe and Russel Kaufman for comments on the manuscript, and Steve Potter, Tom Curran, Judy Grinspan, François Guillemot, Jeffrey Macklis, Tetsuya Taga and Akiya Watanabe for reagents. We also thank the Wistar Microscopy facility for the confocal microscopy images and pictures in Figures 1a–d, and the Wistar Flow Cytometry Facility for help with cortical cell sorting (NIH-NCI Core Grant CA010815). This work was supported by grants from the WW Smith Charitable Trust, the V Foundation, the American Cancer Society (RSG-08-045-01-DDC) and the National Brain Tumor Society to ND.

1. Ever L, Gaiano N. Radial 'glial' progenitors: neurogenesis and signaling. *Curr Opin Neurobiol* 2005; **15**: 29–33.
2. Kriegstein A, Noctor S, Martinez-Cerdeno V. Patterns of neural stem and progenitor cell division may underlie evolutionary cortical expansion. *Nat Rev* 2006; **7**: 883–890.
3. Pontious A, Kowalczyk T, Englund C, Hevner RF. Role of intermediate progenitor cells in cerebral cortex development. *Dev Neurosci* 2008; **30**: 24–32.
4. Kowalczyk T, Pontious A, Englund C, Daza RA, Bedogni F, Hodge R *et al.* Intermediate neuronal progenitors (basal progenitors) produce pyramidal-projection neurons for all layers of cerebral cortex. *Cereb Cortex* 2009; **19**: 2439–2450.
5. Sessa A, Mao CA, Hadjantonakis AK, Klein WH, Broccoli V. Tbr2 directs conversion of radial glia into basal precursors and guides neuronal amplification by indirect neurogenesis in the developing neocortex. *Neuron* 2008; **60**: 56–69.
6. Arnold SJ, Huang GJ, Cheung AF, Era T, Nishikawa S, Bikoff EK *et al.* The T-box transcription factor Eomes/Tbr2 regulates neurogenesis in the cortical subventricular zone. *Genes Dev* 2008; **22**: 2479–2484.
7. Hevner RF. From radial glia to pyramidal-projection neuron: transcription factor cascades in cerebral cortex development. *Mol Neurobiol* 2006; **33**: 33–50.
8. Hevner RF, Hodge RD, Daza RA, Englund C. Transcription factors in glutamatergic neurogenesis: conserved programs in neocortex, cerebellum, and adult hippocampus. *Neurosci Res* 2006; **55**: 223–233.
9. Boland E, Clayton-Smith J, Woo VG, McKee S, Manson FD, Medne L *et al.* Mapping of deletion and translocation breakpoints in 1q44 implicates the serine/threonine kinase AKT3 in postnatal microcephaly and agenesis of the corpus callosum. *Am J Hum Genet* 2007; **81**: 292–303.
10. Hill AD, Chang BS, Hill RS, Garraway LA, Bodell A, Sellers WR *et al.* A 2-Mb critical region implicated in the microcephaly associated with terminal 1q deletion syndrome. *Am J Med Genet* 2007; **143A**: 1692–1698.
11. van Bon BW, Koolen DA, Borgatti R, Magee A, Garcia-Minaur S, Rooms L *et al.* Clinical and molecular characteristics of 1qter microdeletion syndrome: delineating a critical region for corpus callosum agenesis/hypogenesis. *J Med Genet* 2008; **45**: 346–354.
12. Orellana C, Rosello M, Monfort S, Oltra S, Quiroga R, Ferrer I *et al.* Corpus callosum abnormalities and the controversy about the candidate genes located in 1q44. *Cytogenet Genome Res* 2009; **127**: 5–8.
13. Tatard VM, Xiang C, Biegel JA, Dahmane N. ZNF238 is expressed in postmitotic brain cells and inhibits brain tumor growth. *Cancer Res* 2010; **70**: 1236–1246.
14. Aoki K, Meng G, Suzuki K, Takashi T, Kameoka Y, Nakahara K *et al.* RP58 associates with condensed chromatin and mediates a sequence-specific transcriptional repression. *J Biol Chem* 1998; **273**: 26698–26704.
15. Ohtaka-Maruyama C, Miwa A, Kawano H, Kasai M, Okado H. Spatial and temporal expression of RP58, a novel zinc finger transcriptional repressor, in mouse brain. *J Comp Neurol* 2007; **502**: 1098–1108.
16. Okado H, Ohtaka-Maruyama C, Sugitani Y, Fukuda Y, Ishida R, Hirai S *et al.* The transcriptional repressor RP58 is crucial for cell-division patterning and neuronal survival in the developing cortex. *Dev Biol* 2009; **331**: 140–151.
17. Tronche F, Kellendonk C, Kretz O, Gass P, Anlag K, Orban PC *et al.* Disruption of the glucocorticoid receptor gene in the nervous system results in reduced anxiety. *Nat Genet* 1999; **23**: 99–103.
18. Molyneaux BJ, Arlotta P, Menezes JR, Macklis JD. Neuronal subtype specification in the cerebral cortex. *Nat Rev Neurosci* 2007; **8**: 427–437.
19. Bayer SA, Altman J. *Neocortical Development*. Raven Press: New York, 1991.
20. Hevner RF, Shi L, Justice N, Hsueh Y, Sheng M, Smiga S *et al.* Tbr1 regulates differentiation of the preplate and layer 6. *Neuron* 2001; **29**: 353–366.
21. Hartfuss E, Galli R, Heins N, Gotz M. Characterization of CNS precursor subtypes and radial glia. *Dev Biol* 2001; **229**: 15–30.
22. Kawaguchi A, Ikawa T, Kasukawa T, Ueda HR, Kurimoto K, Saitou M *et al.* Single-cell gene profiling defines differential progenitor subclasses in mammalian neurogenesis. *Development* 2008; **135**: 3113–3124.
23. Englund C, Fink A, Lau C, Pham D, Daza RA, Bulfone A *et al.* Pax6, Tbr2, and Tbr1 are expressed sequentially by radial glia, intermediate progenitor cells, and postmitotic neurons in developing neocortex. *J Neurosci* 2005; **25**: 247–251.
24. Gong S, Zheng C, Doughty ML, Losos K, Didkovsky N, Schambra UB *et al.* A gene expression atlas of the central nervous system based on bacterial artificial chromosomes. *Nature* 2003; **425**: 917–925.
25. Kwon GS, Hadjantonakis AK. Eomes::GFP-a tool for live imaging cells of the trophoblast, primitive streak, and telencephalon in the mouse embryo. *Genesis* 2007; **45**: 208–217.
26. Mizutani K, Yoon K, Dang L, Tokunaga A, Gaiano N. Differential Notch signalling distinguishes neural stem cells from intermediate progenitors. *Nature* 2007; **449**: 351–355.
27. Miyata T, Kawaguchi A, Saito K, Kawano M, Muto T, Ogawa M. Asymmetric production of surface-dividing and non-surface-dividing cortical progenitor cells. *Development (Cambridge, England)* 2004; **131**: 3133–3145.
28. Mankinen CB, Hold JG, Sears JW. Partial trisomy 15 in a young girl. *Clin Genet* 1976; **10**: 27–32.
29. Tiveron MC, Hirsch MR, Brunet JF. The expression pattern of the transcription factor Phox2 delineates synaptic pathways of the autonomic nervous system. *J Neurosci* 1996; **16**: 7649–7660.
30. Arlotta P, Molyneaux BJ, Chen J, Inoue J, Kominami R, Macklis JD. Neuronal subtype-specific genes that control corticospinal motor neuron development *in vivo*. *Neuron* 2005; **45**: 207–221.
31. Gradwohl G, Fode C, Guillemot F. Restricted expression of a novel murine atonal-related bHLH protein in undifferentiated neural precursors. *Dev Biol* 1996; **180**: 227–241.
32. Kimura N, Nakashima K, Ueno M, Kiyama H, Taga T. A novel mammalian T-box-containing gene, Tbr2, expressed in mouse developing brain. *Brain Res* 1999; **115**: 183–193.
33. Watakabe A, Ichinohe N, Ohsawa S, Hashikawa T, Komatsu Y, Rockland KS *et al.* Comparative analysis of layer-specific genes in mammalian neocortex. *Cereb Cortex* 2007; **17**: 1918–1933.
34. Lee TI, Johnstone SE, Young RA. Chromatin immunoprecipitation and microarray-based analysis of protein location. *Nat Protocols* 2006; **1**: 729–748.

Supplementary Information accompanies the paper on Cell Death and Differentiation website (http://www.nature.com/cdd)